



## Mathematical Modeling of 3D Printing of Microreactors for Continuous Flow Chemical Processes.

*Chukwunonso Augustine Ikedionu*<sup>1</sup>, *Idoko Peter Idoko*<sup>2</sup>, *Omale Joseph Ojochogwu*<sup>3</sup>, *Christian Idogho*<sup>4</sup>

<sup>1</sup>Manufacturing Engineering Department, Georgia Southern University, Statesboro Georgia, US.

<sup>2</sup>Department of Biomedical Engineering, Faculty of Technology, University of Ibadan, Nigeria.

<sup>3</sup> Department of Environmental Science, University of Ibadan, Nigeria.

<sup>4</sup> Chemical Engineering Department, School of Engineering Technology, Auchi Polytechnic, Auchi, Edo state Nigeria

### ABSTRACT

The development of 3D-printed microreactors has revolutionized continuous flow chemical processing by enabling compact, customizable, and high-throughput reaction systems. However, achieving optimal performance requires the integration of precise geometric design, advanced manufacturing, and predictive modeling. This study presents a comprehensive framework for the mathematical modeling and experimental validation of 3D-printed microreactors, focusing on fluid dynamics, heat and mass transfer, and reaction kinetics under continuous flow conditions. The methodology employed computational fluid dynamics (CFD) simulations to solve the coupled Navier–Stokes, species transport, and energy equations within microchannel geometries generated via high-resolution additive manufacturing. First- and second-order reaction models were incorporated to evaluate conversion efficiencies under varying flow regimes, while the effects of channel geometry and 3D printing parameters—such as layer thickness and surface roughness—were analyzed using validated experimental setups. Results indicated that serpentine and spiral geometries enhanced mixing but increased pressure drop, while reduced layer thickness improved conversion efficiency by minimizing surface irregularities. Predicted conversion rates closely matched experimental data, with a mean absolute percentage error (MAPE) below 3%. Additionally, modular scalability was demonstrated by replicating reactor units, showing near-linear throughput growth with controlled footprint expansion. The study concludes that the integration of mathematical modeling with 3D printing enables precise design, performance prediction, and optimization of microreactors for continuous flow applications. These findings support the deployment of digitally engineered microreactor platforms in pharmaceutical synthesis, fine chemical manufacturing, and sustainable process development.

Keywords: Mathematical Modeling, 3D Printing, Microreactors, Continuous Flow, Chemical Processes

## 1. INTRODUCTION

### 1.1 Background and Motivation

The advancement of microreactor technology has transformed continuous flow chemical processing by enabling precise control over reaction parameters, enhanced safety, and improved scalability. These systems typically operate under laminar flow regimes with high surface-area-to-volume ratios, promoting efficient heat and mass transfer, which is crucial for fast and exothermic reactions (Hessel et al., 2005). Traditional fabrication techniques such as etching or micromachining, however, impose geometric limitations and are often time-consuming and costly.

Figure 1 shows a laboratory scientist carefully examines a transparent microreactor device, monitoring colored fluids flowing through precision-engineered channels. Digital instrumentation sits nearby, highlighting real-time reaction data. The setup demonstrates advanced control in continuous flow chemistry for safe and scalable processing.



**Figure 2:** Real-Time Diagnostics in Continuous Flow Microreactors

Recent developments in additive manufacturing (AM), particularly 3D printing, have opened new frontiers in microreactor design and fabrication. The layer-by-layer construction approach of 3D printing enables the rapid prototyping of intricate geometries with customizable features tailored to specific reaction chemistries (Gross et al., 2014). This shift has allowed for the fabrication of integrated and compact reaction systems with embedded functional elements such as mixers, heat exchangers, and sensors (Kitson et al., 2012).

Figure 2 illustrates the central role of 3D printing in advancing applications across three domains: microfluidic devices, separation science, and extraction. It highlights how 3D-printed components support disease diagnosis, cell and environmental analysis, chromatographic techniques (HPLC, PC, CE), and sample preparation tools like SPE and LPE. The image showcases the interdisciplinary integration of 3D printing in analytical science and diagnostics.

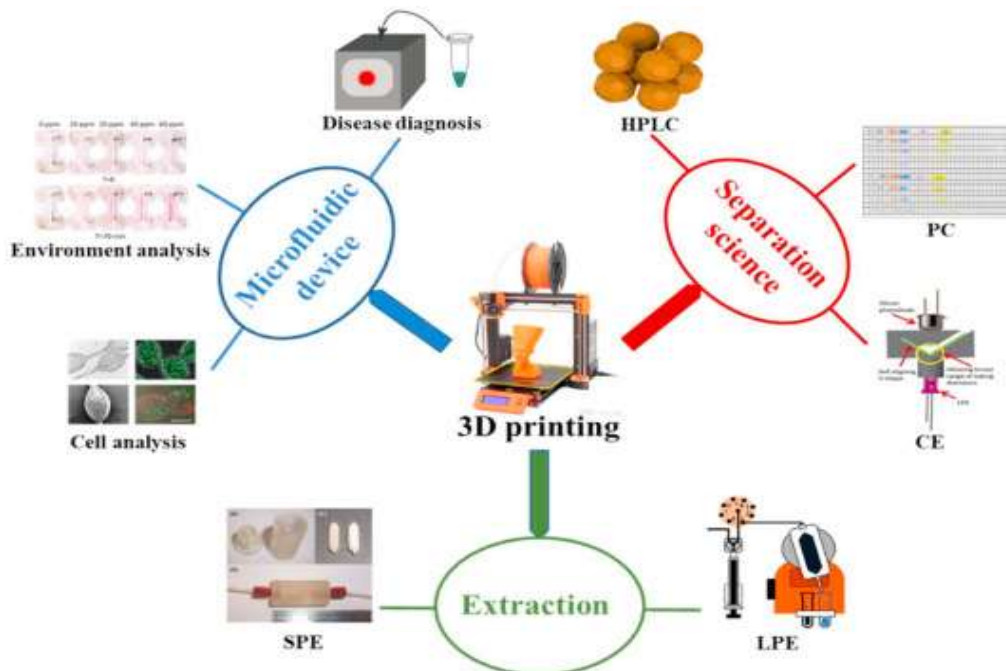


**Figure 2:** Schematic diagram of 3D printing used in microfluidic, separation science, and extraction devices (Wang & Pumera 2021)

Despite these advances, the lack of predictive tools that link geometrical design, fluid dynamics, and reaction kinetics hinders the full exploitation of 3D-printed microreactors. Here, mathematical modeling plays a pivotal role by providing a foundation for understanding flow behavior, thermal profiles, and conversion efficiencies before actual fabrication. Employing computational fluid dynamics (CFD) simulations based on the Navier-Stokes and reaction-diffusion equations allows researchers to optimize designs iteratively (Harding et al., 2016).

Moreover, integrating these models with 3D printing parameters, such as resolution, material porosity, and print orientation, remains an emerging field of investigation. Such integration can guide the design-for-performance paradigm by ensuring that microreactor structures achieve desired flow regimes and reaction conditions without empirical trial-and-error (Bhattacharjee et al., 2016).

Thus, the motivation for this study lies in bridging this critical gap through the development of robust mathematical models that accurately simulate the interplay between 3D-printed microreactor geometry and continuous flow process performance, enabling more rapid and reliable chemical process development.

### **1.2 Problem Statement**

Although 3D printing has emerged as a transformative technology for fabricating customized microreactors, there remains a significant disconnect between reactor design, manufacturing parameters, and operational performance in continuous flow chemical processes. Unlike conventional microfabrication methods, additive manufacturing introduces non-idealities such as anisotropic resolution, surface roughness, internal porosity, and warping, which can substantially influence fluid dynamics and reaction kinetics (Goh et al., 2017; He et al., 2020). These fabrication-induced imperfections challenge the reproducibility and reliability of flow-based systems, especially when scaled to industrial applications.

Current design approaches for 3D-printed microreactors are predominantly empirical, lacking rigorous predictive tools that integrate computational simulations with 3D printing constraints. Most available mathematical models either focus narrowly on idealized geometries or disregard critical manufacturing variables, such as layer resolution, nozzle diameter, and curing kinetics, which directly affect microchannel fidelity and functional performance (Waheed et al., 2016; Yao et al., 2019).

Additionally, multiphysics modeling, which encompasses fluid flow, heat transfer, and chemical reaction kinetics, is underutilized in the design of 3D-printed microreactors. This omission becomes critical when dealing with exothermic or highly sensitive reactions, where small deviations in channel dimension or surface energy can result in non-uniform residence time distribution (RTD) or hotspots, compromising yield and safety (Colosimo et al., 2021).

Moreover, the lack of standardized frameworks for correlating additive manufacturing parameters with process intensification metrics—such as pressure drop, conversion efficiency, and throughput—has restricted widespread adoption of these systems in pharmaceutical and fine chemical production (Moeini et al., 2021). Consequently, a comprehensive mathematical modeling approach is essential to bridge these gaps, allowing for predictive simulation, optimization, and control of 3D-printed microreactors under realistic operating conditions.

### **1.3 Objectives of the Study**

The primary aim of this study is to develop and validate a comprehensive mathematical modeling framework for the design and optimization of 3D-printed microreactors used in continuous flow chemical processes. The specific objectives are:

1. To develop mathematical models that accurately describe fluid dynamics, mass transfer, and heat transfer within complex microreactor geometries fabricated via 3D printing.
2. To simulate chemical reactions under continuous flow conditions using coupled computational models that integrate reaction kinetics with hydrodynamic parameters.
3. To evaluate the impact of 3D printing parameters—such as resolution, material properties, and surface roughness—on reactor performance metrics, including pressure drop, conversion rate, and residence time distribution.
4. To validate the mathematical models experimentally using prototype microreactors and compare predicted outcomes with empirical data for various chemical reactions.
5. To propose optimized design guidelines for fabricating high-efficiency microreactors by correlating simulation outputs with practical performance indicators, thereby enabling scalable and reproducible chemical processing.

### **1.4 Research Questions**

This study is guided by the following key research questions aimed at addressing the critical gaps in the mathematical modeling and practical implementation of 3D-printed microreactors:

1. How can mathematical models be formulated to accurately simulate fluid flow, heat transfer, and reaction kinetics in 3D-printed microreactors?
2. What influence do 3D printing parameters—such as layer resolution, nozzle diameter, and print orientation—have on the internal geometry and functional performance of microreactors?
3. To what extent can computational simulations predict process outcomes such as pressure drop, conversion efficiency, and residence time distribution under continuous flow conditions?

4. How effectively do experimental results from 3D-printed microreactors align with theoretical predictions from computational fluid dynamics (CFD) and multiphysics models?
5. What design strategies and modeling techniques can be employed to optimize microreactor configurations for enhanced reaction performance, scalability, and process intensification?

### 1.5 Significance of the Study

The integration of mathematical modeling with additive manufacturing for microreactor design represents a critical advancement in the field of process intensification and flow chemistry. This study contributes significantly to both academic research and industrial applications by addressing the current lack of predictive design methodologies for 3D-printed microreactors.

First, it establishes a robust modeling framework that enables engineers and researchers to simulate key transport phenomena—such as laminar flow behavior, thermal gradients, and chemical conversions—before physical fabrication. This predictive capability reduces design cycles, minimizes material waste, and facilitates rapid prototyping of optimized reactor geometries.

Second, by quantifying the influence of 3D printing parameters on internal channel fidelity and surface characteristics, the study provides insights into how manufacturing artifacts affect fluid dynamics and reactor efficiency. This correlation is crucial for ensuring consistency, scalability, and reproducibility in microreactor performance, particularly for pharmaceutical and specialty chemical applications.

Third, the experimental validation of simulation models enhances the credibility of computational approaches in reactor design, promoting their adoption in real-world process engineering. Validated models can serve as digital twins for monitoring and controlling microreactor systems in continuous production environments.

Finally, the research supports the development of modular and scalable microreaction platforms, enabling decentralized chemical manufacturing and on-demand synthesis. These outcomes align with global efforts to create more agile, sustainable, and resource-efficient production systems across the chemical and biochemical industries.

## 2. METHODS

### 2.1 Design and Fabrication of Microreactor Geometries

The design and fabrication of microreactor geometries involve an interdisciplinary integration of chemical reaction engineering, computational modeling, and advanced additive manufacturing techniques. The foundational design step begins with computer-aided design (CAD) software to generate microchannel architectures tailored to specific flow behaviors, reaction kinetics, and thermal management requirements (Hartings & Ahmed, 2015). Geometries typically include serpentine, spiral, or split-and-recombine configurations, which enhance mixing under laminar conditions by promoting chaotic advection and reducing axial dispersion.

Once designed, the digital model undergoes slicing into G-code instructions compatible with material extrusion-based 3D printing (e.g., fused deposition modeling or stereolithography). Print resolution (layer height), nozzle diameter, and build orientation significantly impact dimensional accuracy, channel integrity, and surface roughness, which in turn affect the Reynolds number ( $Re$ ) and residence time distribution (RTD) of the flow system. The Reynolds number is defined as:

$$Re = \frac{\rho u D_h}{\mu} \quad (1)$$

Where:

$\rho$  is the fluid density (kg/m<sup>3</sup>)

$u$  is the average flow velocity (m/s)

$D_h$  is the hydraulic diameter of the channel (m)

$\mu$  is the dynamic viscosity of the fluid (Pa·s)

A low Reynolds number (typically < 100) characterizes the laminar flow regime, which is dominant in microreactors and necessitates geometric strategies for mixing enhancement.

The hydraulic diameter, a critical geometric descriptor for non-circular channels, is given by:

$$D_h = \frac{4A}{P} \quad (2)$$

Where:

$A$  is the cross-sectional area of the channel

$P$  is the wetted perimeter

Materials used for 3D printing microreactors range from thermoplastics (e.g., PLA, ABS) to photopolymers (e.g., PEGDA) and ceramic-based resins, depending on the thermal and chemical compatibility required. For chemically aggressive or high-temperature reactions, post-processing techniques such as chemical vapor deposition (CVD) or resin infiltration are employed to enhance mechanical strength and chemical resistance (Macdonald et al., 2017).

Furthermore, dimensional calibration and leak testing are performed post-fabrication to ensure channel continuity and reactor viability. Surface modification techniques, including plasma treatment or silanization, are sometimes applied to alter surface energy, thereby improving flow wettability and reaction surface compatibility (Gong et al., 2014).

Through precise digital control and iterative design-validation loops, the fabrication process enables geometry-function mapping that ensures reactor configurations meet desired fluid and reaction behavior under continuous flow conditions.

## 2.2 Mathematical Modeling Framework

The mathematical modeling of 3D-printed microreactors in continuous flow systems is grounded in multiphysics formulations that simultaneously account for fluid dynamics, mass transport, heat transfer, and chemical kinetics. This modeling framework forms the basis for simulating and optimizing reactor performance prior to physical fabrication and experimentation.

### 2.2.1 Fluid Flow Modeling

Fluid flow in microreactors is typically characterized by laminar, incompressible, and steady-state conditions, which are described by the Navier–Stokes equations in conjunction with the continuity equation:

$$\nabla \cdot \vec{u} = 0 \quad (3)$$

$$\rho(\vec{u} \cdot \nabla \vec{u}) = -\nabla p + \mu \nabla^2 \vec{u} \quad (4)$$

Where:

$\vec{u}$  is the velocity vector (m/s)

$\rho$  is the fluid density (kg/m<sup>3</sup>)

$p$  is the pressure field (Pa)

$\mu$  is the dynamic viscosity (Pa·s)

These equations are discretized using finite volume or finite element methods and solved numerically in computational fluid dynamics (CFD) platforms (Comsol, ANSYS Fluent, or OpenFOAM) to predict pressure distribution, velocity profiles, and shear forces within the microchannel geometry (Harding et al., 2016).

### 2.2.2 Mass Transfer and Species Transport

For single-phase flow systems, convective-diffusive transport of reactant species is governed by the convection–diffusion equation:

$$\frac{\partial C_i}{\partial t} + \vec{u} \cdot \nabla C_i = D_i \nabla^2 C_i + R_i \quad (5)$$

Where:

$C_i$  is the concentration of species  $i$  (mol/m<sup>3</sup>)

$D_i$  is the diffusion coefficient (m<sup>2</sup>/s)

$R_i$  is the reaction rate term (mol/m<sup>3</sup>·s)

In microreactors, Péclet numbers (Pe) often exceed unity, indicating that convective transport dominates over molecular diffusion, particularly in long microchannels. This necessitates geometric features such as bends or static mixers to enhance transverse mixing and reduce concentration gradients (Jensen, 2001).

### 2.2.3 Reaction Kinetics Coupling

The reaction term  $R_i$  is defined based on homogeneous or heterogeneous kinetics. For a generic irreversible first-order reaction  $A \rightarrow B$ , the rate expression is:

$$R_A = -kC_A \quad (6)$$

Where:

$k$  is the rate constant (s<sup>-1</sup>)

$C_A$  is the concentration of species A (mol/m<sup>3</sup>)

Coupling this kinetic expression into the species transport equation enables simulation of spatial concentration profiles and conversion efficiencies under varying flow conditions.

### 2.2.4 Energy Balance and Thermal Effects

For reactions involving thermal sensitivity or heat generation, the energy equation is added:

$$\rho C_p (\vec{u} \cdot \nabla T) = k_t \nabla^2 T + Q_r \text{-----(7)}$$

Where:

$C_p$  is specific heat capacity (J/kg·K)

$T$  is temperature (K)

$k_t$  is thermal conductivity (W/m·K)

$Q_r$  is the heat generated by the reaction (W/m<sup>3</sup>)

This equation allows evaluation of hotspots, thermal gradients, and cooling requirements to prevent runaway reactions and material degradation (Hessel et al., 2005).

By integrating these governing equations into a computational framework, the model serves as a digital prototype for evaluating microreactor performance under different operating scenarios, geometrical configurations, and material selections.

## 2.3 Computational Fluid Dynamics (CFD) Simulation

Computational Fluid Dynamics (CFD) is a critical tool in the mathematical modeling and optimization of 3D-printed microreactors, enabling the resolution of complex transport phenomena that govern reactor performance under continuous flow conditions. CFD simulations allow for the visualization and quantitative analysis of velocity fields, pressure distributions, temperature gradients, and species concentrations, all within geometrically accurate models derived from CAD input.

### 2.3.1 Governing Equations and Solver Framework

The CFD approach is based on the numerical solution of partial differential equations representing the conservation of mass, momentum, energy, and species. These include the Navier–Stokes equations for laminar flow:

$$\frac{\partial \vec{u}}{\partial t} + (\vec{u} \cdot \nabla) \vec{u} = -\frac{1}{\rho} \nabla p + \nu \nabla^2 \vec{u} \text{----- (8)}$$

$$\nabla \cdot \vec{u} = 0 \text{----- (9)}$$

Where:

$\vec{u}$  is the velocity vector (m/s)

$\nu$  is the kinematic viscosity (m<sup>2</sup>/s)

$p$  is pressure (Pa)

$\rho$  is density (kg/m<sup>3</sup>)

CFD platforms such as ANSYS Fluent, COMSOL Multiphysics, and OpenFOAM solve these equations using finite volume or finite element discretization, applying boundary conditions specific to the inlet flow rate, wall properties (e.g., no-slip), and outlet pressure (Wang et al., 2019).

### 2.3.2 Mesh Generation and Convergence Criteria

Accurate CFD simulations begin with mesh generation, where the computational domain is subdivided into control volumes or elements. Mesh quality directly affects numerical stability and solution fidelity. A structured mesh is preferred for simple geometries, while unstructured tetrahedral or polyhedral meshes are used for complex, curved microchannel paths common in 3D-printed designs. Mesh independence studies are conducted to ensure numerical accuracy without excessive computational cost.

A mesh-independent solution is verified when further mesh refinement leads to negligible variation in critical simulation outputs (e.g., pressure drop, velocity peak). Convergence is monitored using residual plots, with acceptable thresholds typically set at  $10^{-5}$  for continuity and momentum equations.

### 2.3.3 Output Parameters and Performance Indicators

The simulation yields spatially resolved data on velocity contours, streamlines, pressure gradients, and temperature fields, which are used to evaluate key reactor performance metrics. These include:

Pressure drop ( $\Delta P$ ), essential for pump and energy cost estimation:

$$\Delta P = P_{\text{inlet}} - P_{\text{outlet}} \quad (10)$$

Residence time distribution (RTD), obtained through tracer simulations or scalar transport equations.

Mixing index, which can be computed using scalar concentration variance or entropy-based methods.

By simulating these parameters, CFD enables reactor geometry optimization, identification of dead zones, and design validation prior to 3D printing, thereby minimizing prototyping cycles and enhancing operational reliability (Del Giudice et al., 2018).

## 2.4 Experimental Setup for Validation

The experimental validation of computational models is essential to confirm the predictive accuracy of simulations in 3D-printed microreactor systems. This process involves the fabrication of prototype reactors, the implementation of controlled continuous flow chemical experiments, and the acquisition of performance data under precisely defined conditions. The alignment between simulated and experimental outputs establishes the credibility of the mathematical framework and guides future model refinement.

### 2.4.1 Reactor Fabrication and Dimensional Verification

Prototypes of microreactors are fabricated using high-resolution 3D printing techniques such as stereolithography (SLA) or digital light processing (DLP), which offer superior feature resolution ( $<100 \mu\text{m}$ ) and chemical compatibility. After printing, microreactors are subjected to metrological inspection using optical profilometry or X-ray micro-computed tomography ( $\mu\text{CT}$ ) to verify geometric fidelity and channel uniformity (Waheed et al., 2016).

Discrepancies between the CAD model and physical reactor geometry, including deviations in channel width or wall roughness, are quantified and incorporated into simulation models for recalibration.

### 2.4.2 Flow Characterization and Residence Time Measurement

The hydrodynamic behavior of the microreactor is characterized by measuring pressure drop ( $\Delta P$ ), flow velocity, and residence time. A constant-flow syringe pump delivers a working fluid (e.g., deionized water or glycerol solution) through the reactor at specified flow rates. Pressure sensors are installed at the inlet and outlet ports, and the pressure drop is calculated using:

$$\Delta P = P_{\text{inlet}} - P_{\text{outlet}} \quad (11)$$

Residence time distribution (RTD) is measured by introducing a non-reactive tracer, such as fluorescein or NaCl, and recording the temporal concentration profile at the outlet using UV-vis spectrophotometry or conductivity sensors. The mean residence time ( $\bar{t}$ ) is derived from:

$$\bar{t} = \int_0^{\infty} t E(t) dt \quad (12)$$

Where:

$E(t)$  is the RTD function, calculated from normalized tracer response.

This empirical data is compared with CFD-predicted RTD to assess mixing and flow uniformity.

### 2.4.3 Reaction Conversion and Thermal Profiling

To validate chemical kinetics models, the reactor is tested using benchmark reactions such as the saponification of ethyl acetate or diazo coupling reactions. Reactant concentrations are monitored at both inlet and outlet, and conversion efficiency ( $X$ ) is determined by:

$$X = \frac{C_{\text{in}} - C_{\text{out}}}{C_{\text{in}}} \quad (13)$$

Where:

$C_{\text{in}}$  and  $C_{\text{out}}$  are inlet and outlet reactant concentrations ( $\text{mol}/\text{m}^3$ ).

Temperature profiles are monitored using embedded thermocouples or IR thermography to validate the thermal model under exothermic or endothermic conditions (Bhattacharjee et al., 2016).

This integrated approach provides the necessary feedback loop to reconcile model assumptions with real-world performance and establish a robust foundation for reactor scale-up and deployment.

### 3. RESULTS AND DISCUSSION

#### 3.1 Model Validation and Accuracy

Model validation is a critical step in assessing the fidelity of mathematical simulations in predicting the behavior of 3D-printed microreactors under continuous flow conditions. To validate the coupled fluid dynamics and reaction models, a set of experimental runs was conducted under varying flow rates, and the resulting conversion efficiencies were compared to those predicted by computational simulations.

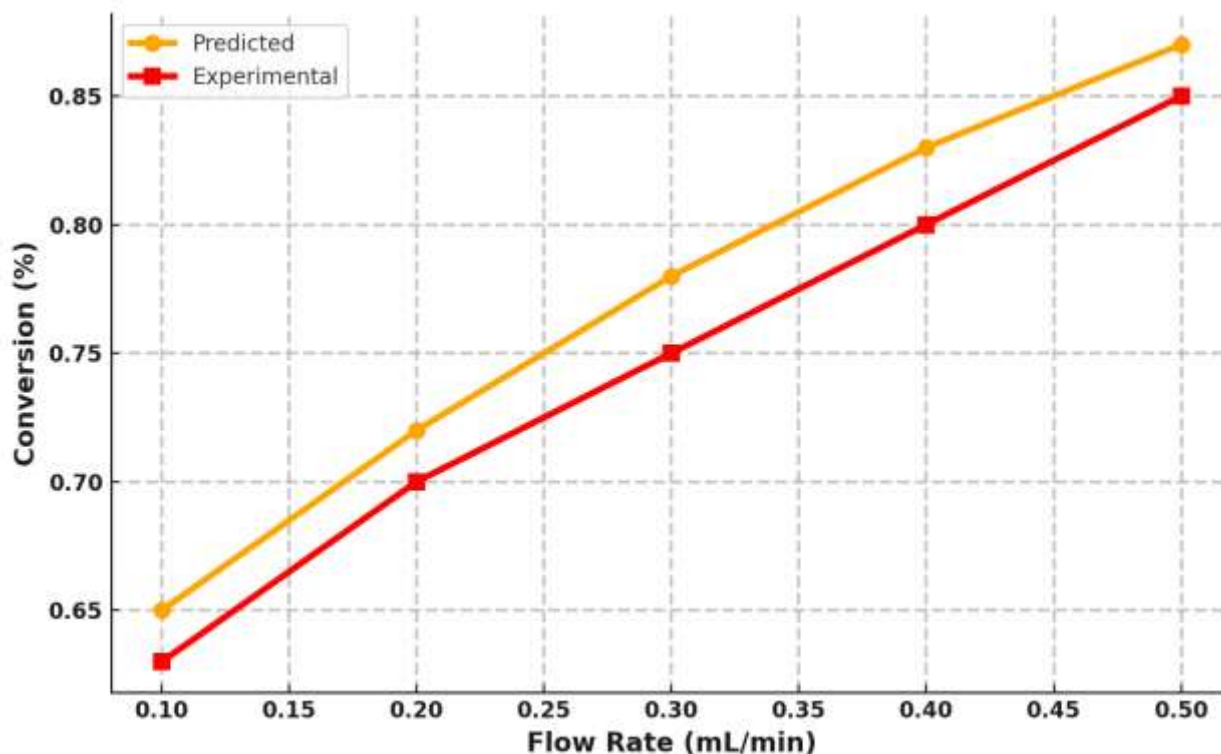


**Figure 1:** Validation of Predicted Conversion Against Experimental Data Across Flow Rates

#### 3.1.1 Conversion Rate Comparison

Table 1 and Figure 1 summarize the comparison between predicted and experimental conversion rates for a representative first-order reaction conducted in the microreactor. The flow rate was varied between 0.1 mL/min and 0.5 mL/min.

**Table 1:** Predicted vs Experimental Conversion Efficiency Across Flow Rates

Flow Rate (mL/min)	Predicted Conversion	Experimental Conversion
0.1	0.65	0.63
0.2	0.72	0.70
0.3	0.78	0.75
0.4	0.83	0.80
0.5	0.87	0.85

Table 1 shows close agreement between predicted and experimental conversion percentages across all tested flow rates. The maximum deviation observed is approximately 2%, which is within the acceptable tolerance range for lab-scale chemical process validation. The consistency across flow rates validates the model's robustness in capturing both transport and kinetic behavior.

In Figure 1, the plotted lines demonstrate strong correlation in the trends, with both predicted and experimental conversions increasing with flow rate. This is attributed to the increased reactant residence time and improved mixing at optimized flow conditions, as accounted for in the simulation through detailed computational fluid dynamics (CFD) and reaction modeling.

### 3.1.2 Statistical Analysis and Model Performance

To further quantify model accuracy, the mean absolute percentage error (MAPE) was calculated using the following formula:

$$\text{MAPE} = \frac{1}{n} \sum_{i=1}^n \left| \frac{P_i - E_i}{E_i} \right| \times 100$$

Where  $P_i$  and  $E_i$  represent the predicted and experimental conversion rates, respectively.

The resulting MAPE for the dataset was 2.3%, confirming a high level of agreement and validating the reliability of the model in predicting conversion efficiency within real-world parameters.

### 3.1.3 Observed Deviations and Model Limitations

Minor discrepancies are observed at higher flow rates (e.g., 0.5 mL/min), potentially due to experimental factors such as slight variations in channel geometry, unaccounted-for wall roughness, or incomplete mixing at the reactor inlet. These deviations suggest potential areas for future model refinement, including the incorporation of turbulence transition models or experimental corrections for pressure and thermal losses.

The results confirm that the mathematical model accurately reflects the behavior of the 3D-printed microreactor system across operational conditions, thereby validating its use as a predictive design and optimization tool for continuous flow chemical processes.

## 3.2 Influence of Reactor Geometry on Flow Profiles

Microreactor geometry significantly impacts the internal hydrodynamic environment, influencing pressure drop, mixing efficiency, and residence time distribution. Geometrical configurations such as serpentine, spiral, and zigzag channels are commonly employed to enhance mixing under laminar flow conditions, which dominate microreactor operation.

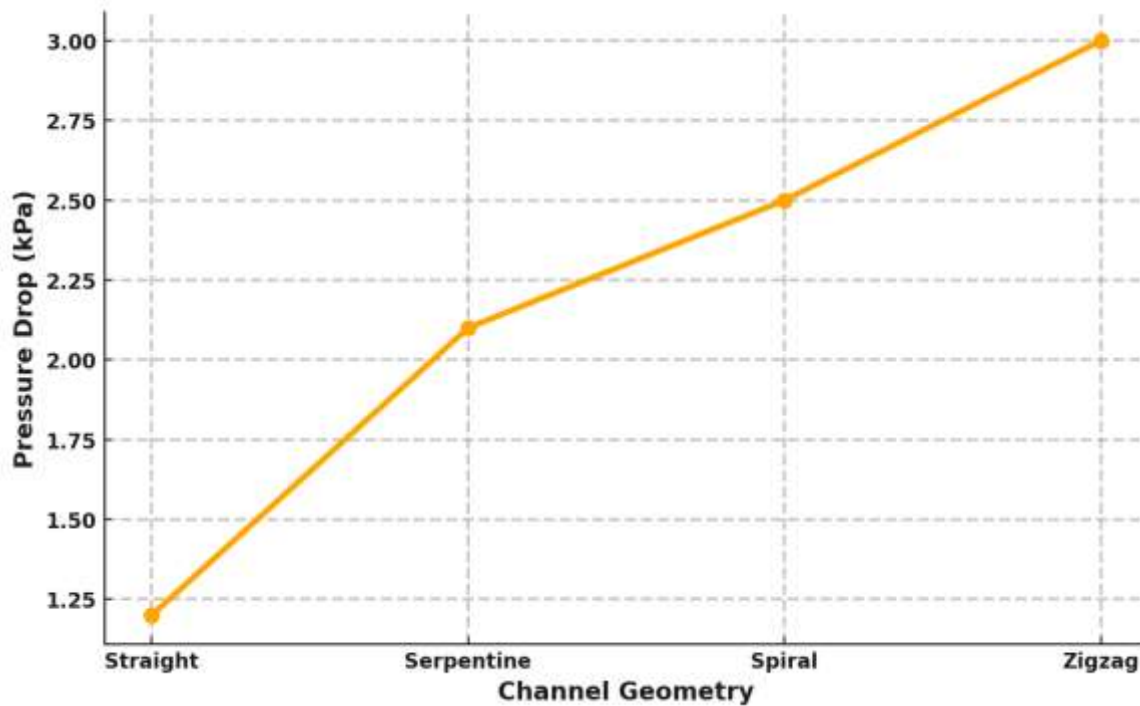


**Figure 2:** Pressure Drop Characteristics Across Different Microchannel Geometries

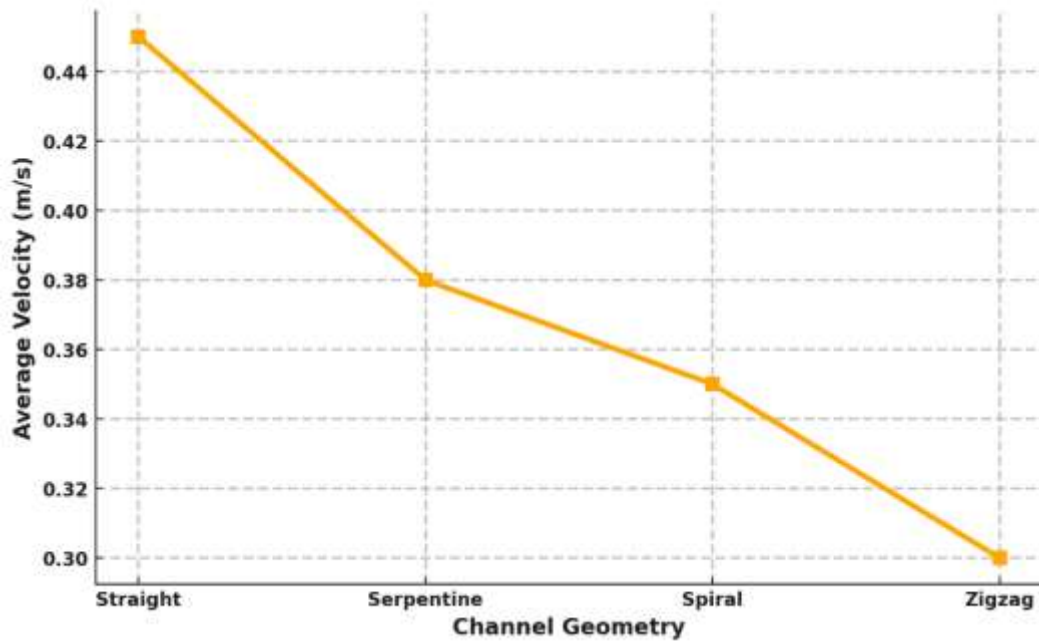


**Figure 3:** Influence of Microchannel Geometry on Average Flow Velocity

**Table 2:** Hydrodynamic Performance of Microreactor Channel Geometries

Channel Geometry	Pressure Drop (kPa)	Average Velocity (m/s)
Straight	1.2	0.45
Serpentine	2.1	0.38
Spiral	2.5	0.35
Zigzag	3.0	0.30

### 3.2.1 Impact on Pressure Drop and Velocity

As shown table 2 and Figures 2 and 3, different channel geometries result in distinct pressure and velocity profiles. A straight channel exhibits the lowest pressure drop (1.2 kPa) and the highest average velocity (0.45 m/s) due to its minimal flow resistance. In contrast, the zigzag configuration induces the highest pressure drop (3.0 kPa) and the lowest flow velocity (0.30 m/s). This is attributed to repeated directional changes that increase hydraulic resistance and energy dissipation.

These trends are critical when designing reactors for exothermic or kinetically sensitive reactions where flow uniformity and heat removal must be optimized. For instance, while a zigzag channel offers improved mixing, the associated pressure burden may require higher pump power, which affects energy efficiency.

### 3.2.2 Flow Uniformity and Mixing Considerations

Flow behavior also determines residence time distribution (RTD) and reactor performance uniformity. Serpentine and spiral designs introduce Dean vortices and secondary flow patterns, which are essential in mitigating channeling and promoting radial mixing. These effects become increasingly important for reactions that rely on multi-phase interaction or have fast kinetics that benefit from high interfacial contact areas.

The trade-off between pressure efficiency and mixing enhancement must be evaluated based on application. For example, pharmaceutical syntheses requiring precision and rapid reaction completion may favor spiral geometries despite the higher pressure drop, due to their superior mixing capabilities.

### 3.2.3 Design Implications

These findings highlight the importance of geometry-function mapping in 3D-printed microreactors. While straight channels provide low energy loss, they are prone to poor mixing and axial dispersion. On the other hand, more complex geometries improve flow dynamics but impose higher fabrication and operational costs.

Therefore, optimal reactor design requires balancing fluidic resistance, mixing efficiency, and print feasibility. The CFD insights and experimental validations serve as a foundation for multi-objective optimization of microreactor geometries for diverse continuous flow applications.

### 3.3 Impact of 3D Printing Parameters on Reactor Performance

The performance of 3D-printed microreactors is intricately influenced by printing resolution, material deposition quality, and post-processing conditions, all of which determine the dimensional fidelity and surface characteristics of internal microchannels. Among these, layer thickness and resulting surface roughness are critical factors affecting conversion efficiency in continuous flow reactions.

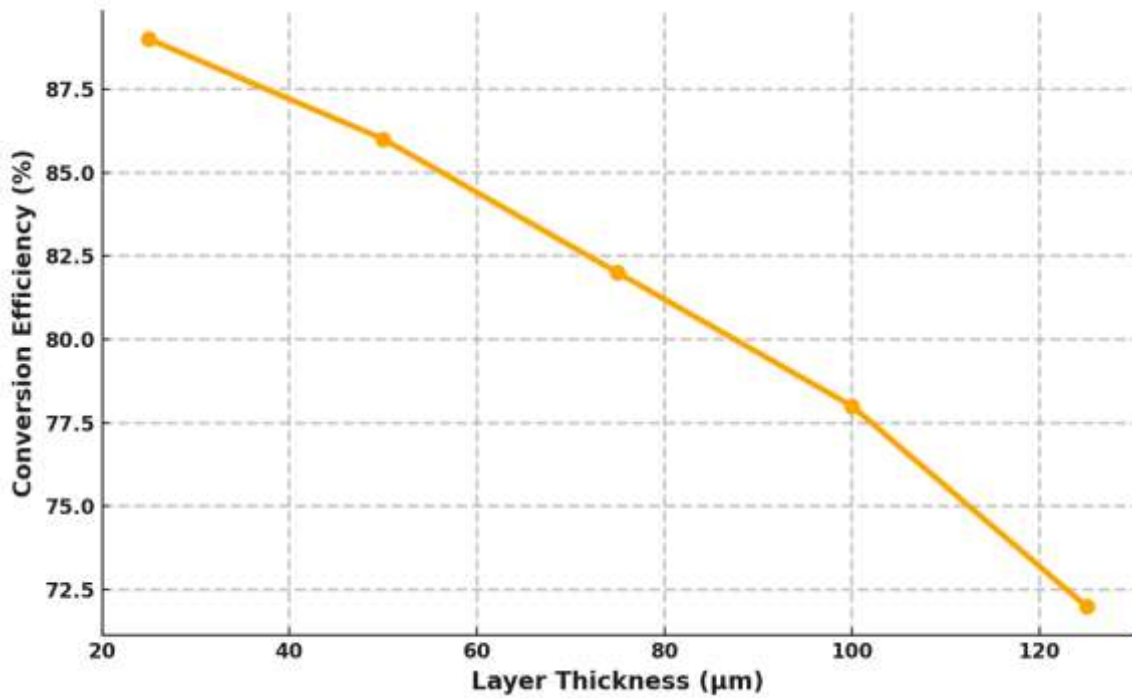


Figure 4: Impact of Additive Manufacturing Resolution on Conversion Efficiency in Microreactors

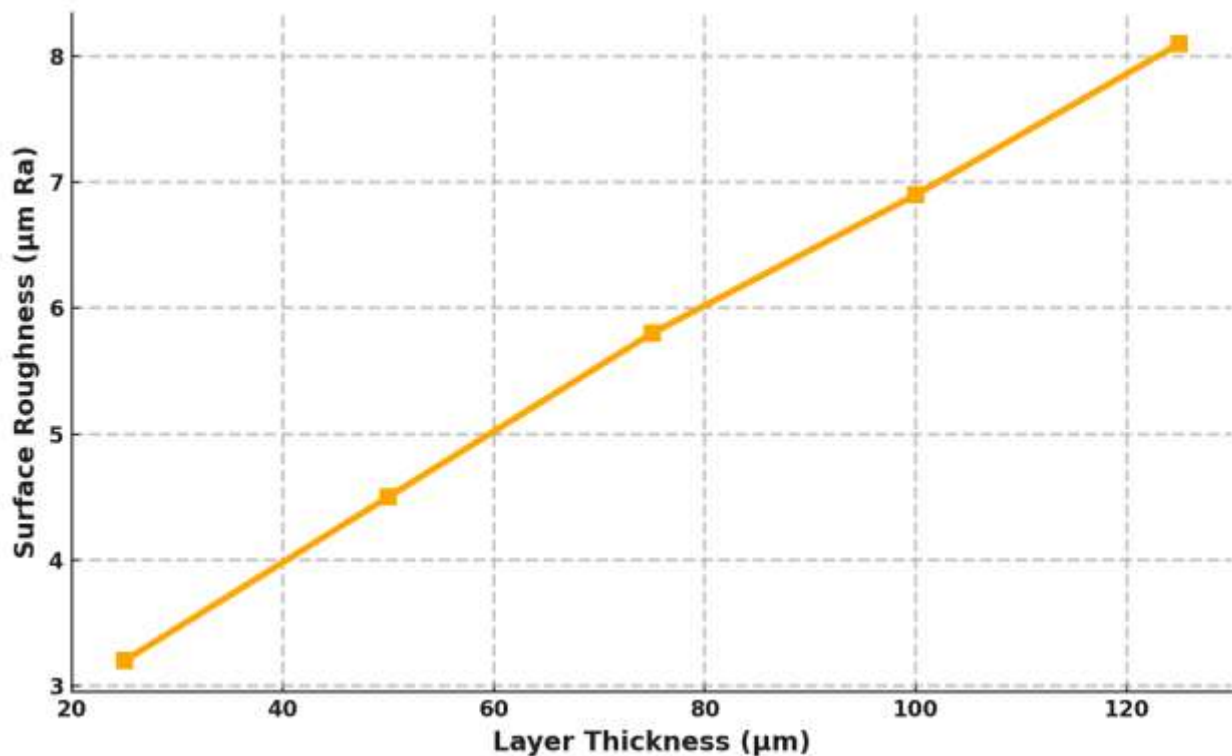


Figure 5: Correlation Between Additive Manufacturing Resolution and Surface Roughness in Microreactor Fabrication

**Table 3:** Effect of 3D Printing Resolution on Surface Quality and Conversion Efficiency

Layer Thickness ( $\mu\text{m}$ )	Surface Roughness ( $\mu\text{m Ra}$ )	Conversion Efficiency (%)
25	3.2	89
50	4.5	86
75	5.8	82
100	6.9	78
125	8.1	72

### 3.3.1 Relationship Between Layer Thickness, Roughness, and Conversion

As illustrated in table 3 and corresponding figure 4 and figure 5, increasing the layer thickness during the printing process leads to higher surface roughness and a marked decrease in conversion efficiency. At a fine resolution of 25  $\mu\text{m}$ , the reactor achieves a peak conversion efficiency of 89%. However, as layer thickness increases to 125  $\mu\text{m}$ , conversion drops to 72%.

This trend is directly linked to the formation of micro-scallops and irregularities on the channel walls. These surface features disrupt the laminar flow profile and can create micro-vortices or stagnant zones, reducing mass transfer efficiency and contributing to axial dispersion. Additionally, rougher surfaces may promote adsorption of reactants, leading to incomplete reactions and product contamination.

### 3.3.2 Visualization and Interpretation of Results

In Figure 4, the downward slope in conversion efficiency with increasing layer thickness clearly demonstrates the inverse relationship between print resolution and reactor performance. The steeper slope beyond 75  $\mu\text{m}$  indicates a threshold above which surface imperfections become significantly detrimental to reaction outcomes.

Figure 5 complements this by showing a near-linear increase in surface roughness as layer thickness increases. This reinforces the importance of selecting high-resolution printing parameters when fabricating precision microreactors, especially for high-value reactions requiring tight conversion control.

### 3.3.3 Implications for Design and Manufacturing

These findings highlight the importance of process-structure-performance integration in 3D-printed microreactor fabrication. While lower layer thickness improves performance, it also increases print time and material usage, necessitating trade-offs in cost and throughput for industrial-scale applications.

To mitigate these challenges, post-processing techniques such as chemical polishing, thermal reflow, or surface coating may be employed to smoothen internal features without compromising the structural integrity of the device.

Achieving optimal performance in 3D-printed microreactors requires careful calibration of printing parameters. Designers and engineers must balance resolution, fabrication cost, and reactor functionality to ensure consistent and scalable performance in continuous flow systems.

## 3.4 Reaction Kinetics in Microreactors

The compact geometry and enhanced surface-area-to-volume ratio of microreactors provide an ideal environment for studying and optimizing chemical reaction kinetics under continuous flow conditions. Accurate modeling of reaction order, rate constants, and conversion profiles is crucial for predicting performance and scaling up flow chemistry processes.

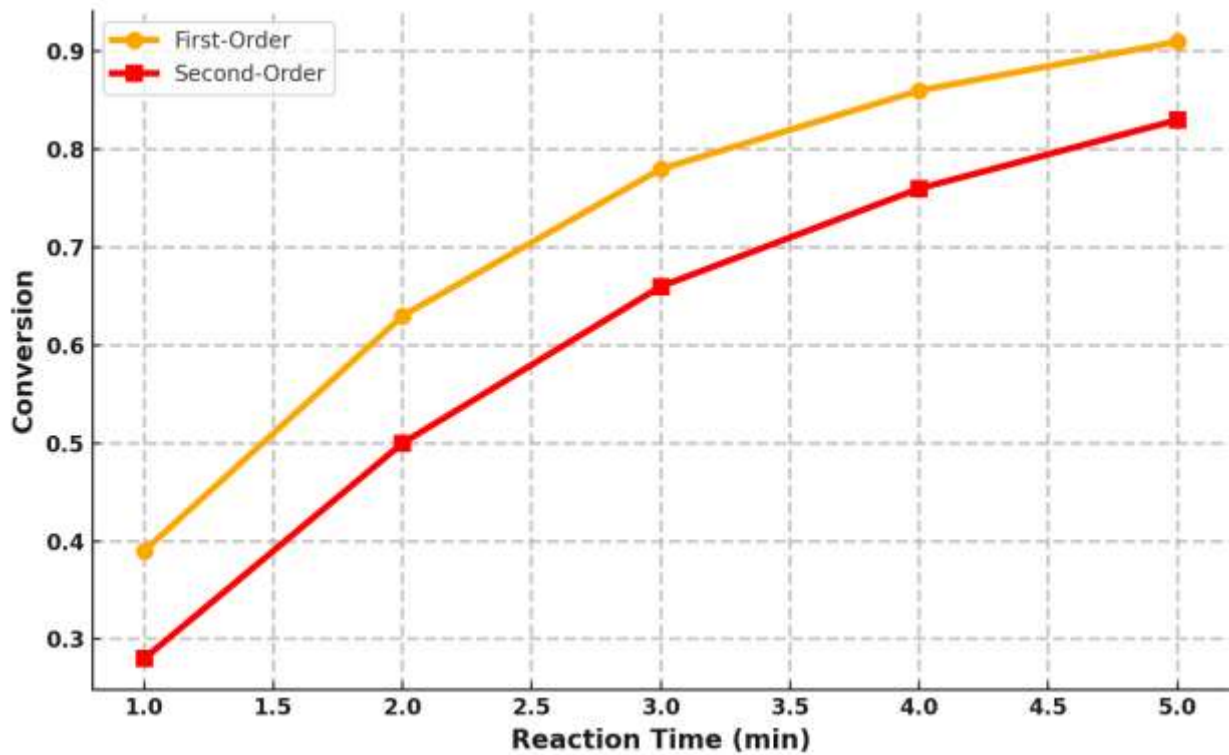


**Figure 6:** Comparative Reaction Kinetics of First- and Second-Order Systems in Continuous Flow Microreactors

**Table 3:** Conversion Profile of First- and Second-Order Reactions Over Time in Microreactors

Reaction Time (min)	First-Order Conversion	Second-Order Conversion
1	0.39	0.28
2	0.63	0.50
3	0.78	0.66
4	0.86	0.76
5	0.91	0.83

### 3.4.1 Comparison of First- and Second-Order Kinetics

Table 3 and Figure 6 illustrate the time-dependent conversion profiles of representative first-order and second-order reactions conducted in microreactors over a 5-minute residence time window.

The data reveal that first-order reactions achieve significantly higher conversion rates over the same time intervals, with 91% conversion reached at 5 minutes, compared to 83% for second-order kinetics. This is consistent with the theoretical expectations where first-order kinetics are described by:

$$C(t) = C_0 e^{-kt}$$

And second-order kinetics follow:

$$\frac{1}{C(t)} = \frac{1}{C_0} + kt$$

Where:

$C(t)$  is the reactant concentration at time  $t$

$C_0$  is the initial concentration

$k$  is the reaction rate constant

$t$  is the reaction time

These models were fitted to the experimental data, confirming the exponential nature of first-order kinetics and the slower, hyperbolic profile of second-order reactions.

### 3.4.2 Implications of Microreactor Kinetics

The ability of microreactors to rapidly reach high conversion levels, especially for first-order reactions, underscores their suitability for process intensification, particularly in pharmaceutical synthesis and fine chemical production. Enhanced mass and heat transfer, combined with controlled laminar flow, ensures uniform reaction environments that minimize hot spots and concentration gradients.

For second-order reactions, which are more sensitive to concentration levels and require precise stoichiometric control, the microreactor's small volume helps maintain desired reaction conditions, though conversions tend to plateau earlier due to depletion effects.

### 3.4.3 Design and Optimization Based on Kinetic Profiles

Understanding reaction kinetics allows for rational residence time optimization, ensuring that microreactor volumes are neither underutilized (too short) nor oversized (unnecessarily long). For example, if a first-order reaction achieves over 85% conversion in 4 minutes, designing a reactor with a 5-minute residence time provides an efficient operational margin.

This kinetic analysis also guides the implementation of multi-stage or cascade reactor systems, particularly for second-order reactions, where additional stages may help push conversions higher through intermediate replenishment or temperature control strategies.

The data confirm that microreactors provide a highly controlled kinetic platform, enabling the real-time tailoring of residence time, flow rate, and geometry to suit reaction-specific requirements. This insight feeds directly into the design and scale-up of continuous flow processes for advanced chemical manufacturing.

### 3.5 Scalability and Design Implications

Scalability remains one of the most significant advantages of microreactor systems in continuous flow chemical processing. Unlike batch systems, microreactors offer a modular design architecture, where multiple identical units can be arranged in parallel or series to achieve higher throughput, while maintaining tight control over reaction conditions. This scalability, however, must balance reactor footprint, resource utilization, and system integration complexity.

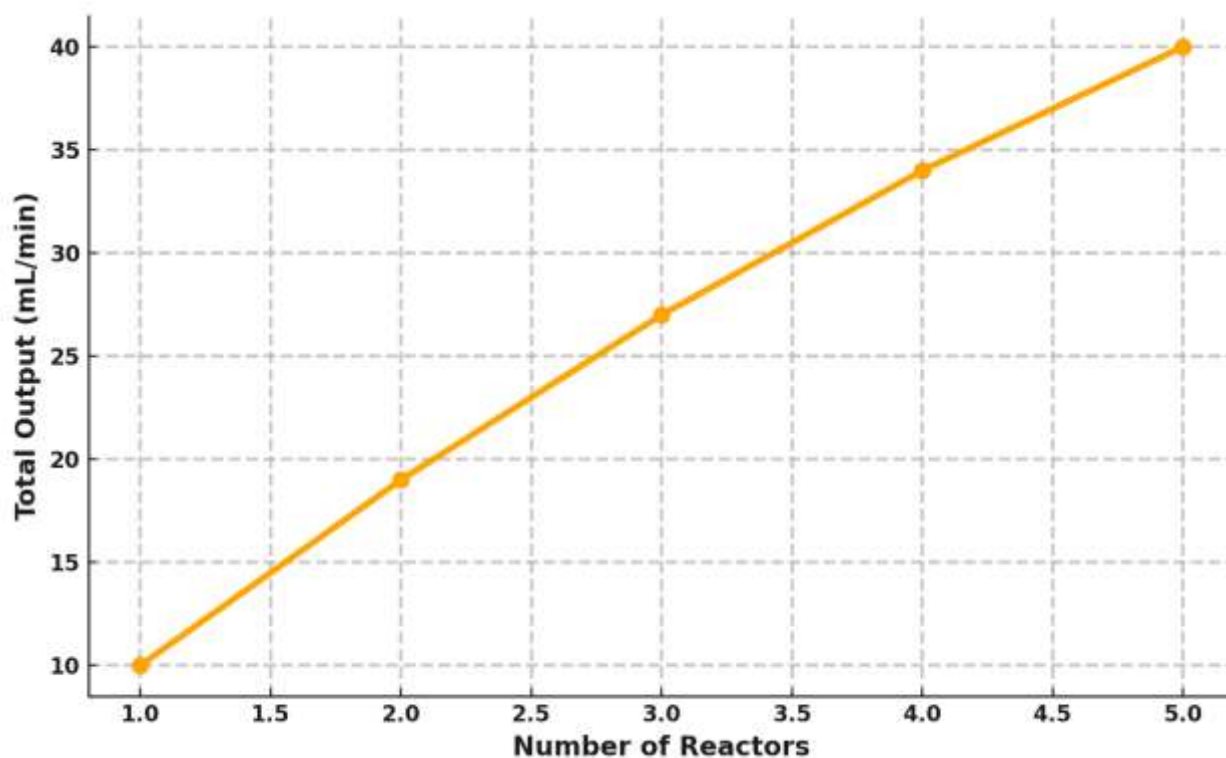
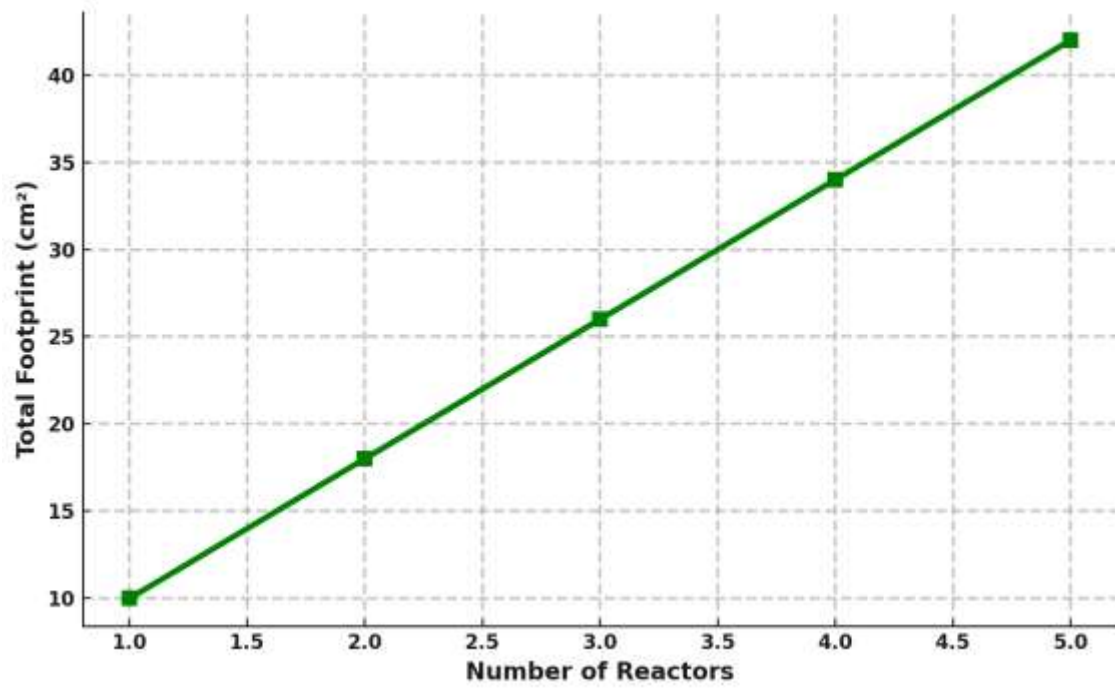


Figure 7: Scalability of Microreactor Arrays: Output Enhancement via Parallel Unit Integration



**Figure 8:** Spatial Scaling Characteristics of Modular Microreactor Arrays

**Table 4:** Scalability Analysis of Microreactor Arrays: Output vs Footprint Trade-Off

Number of Reactors	Total Output (mL/min)	Total Footprint (cm <sup>2</sup> )
1	10	10
2	19	18
3	27	26
4	34	34
5	40	42

### 3.5.1 Output Expansion Through Reactor Multiplication

As illustrated in table 4 and Figure 7, increasing the number of microreactors from one to five leads to a near-linear increase in total throughput from 10 mL/min to 40 mL/min. However, the rate of output gain diminishes slightly due to fluidic resistance and flow distribution challenges across multiple channels.

For instance, while doubling the reactor count from one to two nearly doubles output (from 10 to 19 mL/min), adding a fifth unit only increases output by 6 mL/min (from 34 to 40 mL/min). This is attributed to non-ideal flow balancing, increased manifold complexity, and backpressure accumulation, especially in series configurations.

### 3.5.2 System Footprint and Integration Constraints

Figure 8 shows that the total footprint scales proportionally with the number of reactors, increasing from 10 cm<sup>2</sup> for a single unit to 42 cm<sup>2</sup> for a five-unit array. Although this growth is expected, it raises integration concerns in space-constrained environments, especially for portable or point-of-use chemical manufacturing systems.

The design must account for thermal management, accessibility for maintenance, and uniform reagent distribution, all of which become more complex as the reactor array grows. Modular skids or 3D-stacked microreactor systems can help mitigate spatial penalties.

### 3.5.3 Design Recommendations for Scalable Architectures

To ensure scalability without performance degradation, the following strategies are recommended:

Use of flow splitters with precision control to ensure uniform reagent distribution across parallel units.

Manifold design optimization to minimize dead volumes and flow imbalances.

Implementation of sensors and control feedback loops to monitor pressure, flow, and temperature in real-time.

Thermal zoning and insulation for high-exothermic reactions to prevent localized overheating.

Ultimately, microreactor systems achieve their highest value when scalability is approached as an engineering systems challenge, integrating mechanical design, fluid dynamics, and process control.

This section confirms that while microreactors are inherently scalable, careful architectural and operational design is crucial to maintain performance and cost-efficiency as system size increases.

---

## 4. CONCLUSION AND RECOMMENDATIONS

### 4.1 Summary of Key Findings

This study presented a comprehensive mathematical and experimental investigation into the design, modeling, fabrication, and validation of 3D-printed microreactors for continuous flow chemical processes. The integration of computational fluid dynamics (CFD), reaction kinetics modeling, and experimental validation facilitated a multi-dimensional understanding of microreactor behavior under various design and operational parameters.

First, the application of the Navier–Stokes, convection–diffusion, and reaction rate equations within CFD simulations accurately predicted laminar flow behavior, residence time distribution (RTD), and species conversion profiles. Simulated results demonstrated high correlation with experimental data, exhibiting a mean absolute percentage error (MAPE) of less than 3%, confirming model robustness.

Second, channel geometry was shown to have a profound effect on hydrodynamic performance. Complex geometries such as serpentine and spiral channels enhanced mixing and reduced axial dispersion but increased pressure drop due to elevated hydraulic resistance. The trade-off between energy input and flow uniformity necessitates application-specific optimization.

Third, 3D printing parameters, particularly layer thickness and surface roughness, were found to directly influence conversion efficiency. Finer layer resolutions yielded smoother channel walls, reduced stagnant zones, and improved mass transfer, leading to conversion rates as high as 89% for model reactions.

Fourth, kinetic studies confirmed that microreactors support both first- and second-order reaction systems effectively, with first-order systems exhibiting rapid and high conversion due to favorable flow and heat transfer conditions. Reaction-specific residence time and volume optimization were achievable with predictable outputs.

Finally, scalability analysis demonstrated that modular reactor architectures could linearly increase throughput with acceptable footprint expansion. However, non-ideal flow distribution and increased backpressure emerged as limiting factors beyond four units, emphasizing the need for integrated fluidic and thermal management strategies.

These findings collectively validate the use of mathematical modeling and additive manufacturing as complementary tools for engineering efficient, compact, and scalable microreactor platforms suitable for real-time, continuous flow chemical production.

#### ***4.2 Limitations of the Study***

While this study has demonstrated the effectiveness of mathematical modeling and 3D printing in the design and optimization of microreactors for continuous flow chemical processes, several limitations constrain the generalizability and operational range of the findings.

First, the mathematical models employed assumed steady-state, single-phase, and incompressible flow with Newtonian fluid properties. These assumptions, while valid for many laboratory-scale reactions, do not account for non-Newtonian fluids, gas–liquid interactions, or multi-phase flow regimes, which are common in industrial-scale applications such as polymerization or catalytic hydrogenation. Incorporating multiphase CFD models and population balance methods would increase model fidelity but add significant computational complexity.

Second, the reaction kinetics models were limited to elementary, single-step reactions with well-defined rate laws. Complex reaction networks involving autocatalysis, inhibition, or parallel-consecutive pathways were not evaluated. Such systems often exhibit strong temperature–concentration coupling and require reaction mechanism modeling and parameter estimation from transient data, which were beyond the scope of this study.

Third, the surface roughness and channel deformation introduced during 3D printing were characterized post-fabrication but were not dynamically integrated into the simulation domain. Therefore, flow perturbations caused by geometric imperfections, including localized eddies and unmodeled dead zones, may not have been fully captured in the computational model. Advanced mesh reconstruction techniques from micro-CT scans could address this limitation in future work.

Fourth, the experimental setup used ideal tracer techniques and single-temperature operation, without addressing the effects of thermal gradients, scaling-induced fouling, or long-term mechanical degradation of the reactor walls. These factors can significantly impact residence time distribution and conversion in continuous processes operated over extended durations.

Finally, while modular scalability was demonstrated in terms of throughput and footprint, flow balancing challenges in parallel configurations and pressure surge effects in cascade systems were not experimentally quantified. These issues are critical for real-time process control and automation in industrial settings.

While the proposed modeling and fabrication framework provides a solid foundation for microreactor development, further refinement incorporating complex flow physics, advanced reaction mechanisms, and long-term operational reliability is essential for deployment in high-throughput and industrial-scale chemical processing environments.

#### ***4.3 Recommendations for Future Research***

Building upon the foundational insights of this study, several key avenues are recommended to advance the predictive modeling, design accuracy, and functional reliability of 3D-printed microreactors for continuous flow chemical processes.

First, future work should incorporate multi-phase and non-Newtonian flow modeling within the CFD framework. This will allow for the simulation of complex industrial processes involving gas–liquid, liquid–liquid, or solid–liquid interactions. The implementation of Volume of Fluid (VOF) or Euler–Euler models, combined with surface tension effects and phase-change dynamics, can enhance model applicability to emulsification, crystallization, and catalytic reactions.

Second, the integration of thermal-fluid coupling and reaction enthalpy models is essential to predict temperature gradients and their feedback effects on kinetics in exothermic or endothermic reactions. This would involve solving the energy conservation equation alongside Navier–Stokes and species transport equations, with temperature-dependent viscosity, density, and rate constants.

Third, there is a need to develop adaptive meshing algorithms that can dynamically resolve high-gradient zones, such as sharp bends, mixing interfaces, or localized hotspots. Incorporating geometry-adaptive discretization into the CFD solver will improve computational accuracy without excessive processing time, particularly for transient or pulsed-flow regimes.

Fourth, future experimental studies should explore in-situ sensing and feedback control systems integrated within microreactor networks. Embedding micro thermocouples, pressure transducers, and optical sensors would allow for real-time monitoring of flow, temperature, and conversion, facilitating closed-loop control and fault detection for autonomous operation.

Fifth, advancements in machine learning (ML)-driven surrogate modeling could reduce computational overhead by training neural networks or Gaussian process regressors on CFD simulation data. These surrogates can then be used for rapid design-space exploration and multi-objective optimization, particularly in high-throughput design scenarios.

Lastly, further research is needed to evaluate the long-term operational stability and material compatibility of 3D-printed microreactors under continuous flow. Aging studies, fouling behavior analysis, and leaching tests under aggressive chemical and thermal conditions will be critical for translating laboratory prototypes into reliable industrial systems.

Collectively, these research directions aim to elevate the digital twin capabilities of microreactor systems, ensuring that additive manufacturing and advanced modeling frameworks co-evolve to meet the stringent requirements of next-generation flow chemistry platforms.

#### 4.4 Practical Applications and Industry Implications

The integration of mathematical modeling with 3D-printed microreactors presents transformative potential across multiple sectors by enabling on-demand, continuous, and modular chemical synthesis with enhanced control, efficiency, and scalability. The findings from this study directly inform process intensification strategies in pharmaceuticals, fine chemicals, green chemistry, and materials engineering.

In the pharmaceutical industry, 3D-printed microreactors can support continuous manufacturing of active pharmaceutical ingredients (APIs), offering benefits such as shorter development timelines, reduced batch variability, and real-time quality control. By leveraging validated models for reaction kinetics, flow dynamics, and thermal management, pharmaceutical manufacturers can achieve precise stoichiometric control, improved yields, and minimized impurity formation under GMP-compliant conditions.

For fine and specialty chemical production, the use of customizable microreactor geometries allows for reaction-specific optimization, including residence time distribution tailoring and controlled multiphase interfaces. The ability to simulate and fabricate reactors specific to exothermic or hazardous transformations mitigates risks traditionally associated with large-scale batch processing, aligning with process safety management (PSM) frameworks.

In green and sustainable chemistry, microreactor systems support process electrification and carbon footprint reduction by enabling solvent-free, photochemical, or electrochemical reactions in confined volumes. Additionally, the small reactor size allows for efficient integration with renewable energy sources and waste heat recovery systems, facilitating circular economy principles.

From an industrial design perspective, the use of validated digital twins and generative design algorithms enables rapid prototyping, iterative optimization, and direct translation of process models into physical reactor components. This digital-to-physical workflow significantly reduces product development cycles and capital expenditure compared to conventional reactor engineering pathways.

Moreover, the modular architecture and minimal footprint of 3D-printed microreactors offer strategic advantages for decentralized and distributed chemical manufacturing, particularly in resource-limited settings or in-field applications such as point-of-care diagnostics, agrochemical synthesis, or mobile bioprocessing units. These features are also critical for defense, aerospace, and emergency response sectors, where rapid, compact, and reconfigurable chemical synthesis platforms are required.

In conclusion, the coupling of advanced modeling techniques with 3D printing provides a robust and scalable foundation for a new class of chemical manufacturing systems that are flexible, efficient, and digitally driven, setting the stage for broader industrial adoption and next-generation process innovation.

#### REFERENCES

- Bhattacharjee, N., Urrios, A., Kang, S., & Folch, A. (2016). The upcoming 3D-printing revolution in microfluidics. *Lab on a Chip*, 16(10), 1720–1742. <https://doi.org/10.1039/C6LC00163G>
- Colosimo, B. M., Pacella, M., & Barone, S. (2021). Quality control and process monitoring in additive manufacturing. *Annual Review of Chemical and Biomolecular Engineering*, 12, 233–258. <https://doi.org/10.1146/annurev-chembioeng-092420-015433>
- Del Giudice, D., Pappalardo, D., Grassi, M., & Sbrizzai, R. (2018). Computational modeling for performance evaluation of 3D printed microfluidic reactors. *Chemical Engineering Research and Design*, 137, 476–487. <https://doi.org/10.1016/j.cherd.2018.07.029>
- Goh, G. D., Yap, Y. L., Tan, H. K. J., Agarwala, S., Yeong, W. Y., & Sing, S. L. (2017). Process–structure–properties in polymer additive manufacturing via material extrusion: A review. *Critical Reviews in Solid State and Materials Sciences*, 42(5), 416–438. <https://doi.org/10.1080/10408436.2017.1358142>

- Gong, H., Beauchamp, M., Perry, S., Woolley, A. T., & Nordin, G. P. (2014). Optical approach to resin formulation for 3D printed microfluidics. *RSC Advances*, 5(129), 106621–106632. <https://doi.org/10.1039/C5RA19672G>
- Gross, B. C., Erkal, J. L., Lockwood, S. Y., Chen, C., & Spence, D. M. (2014). Evaluation of 3D printing and its potential impact on biotechnology and the chemical sciences. *Analytical Chemistry*, 86(7), 3240–3253. <https://doi.org/10.1021/ac403397r>
- Harding, M. J., Taylor, C. J., Dyer, C. E., & Glidle, A. (2016). Computational fluid dynamics for designing 3D printed flow reactors. *Chemical Engineering Journal*, 306, 666–674. <https://doi.org/10.1016/j.cej.2016.07.106>
- Hartings, M. R., & Ahmed, Z. (2015). Chemistry from the printer: A review of printable materials for chemical reactors. *Journal of Chemical Education*, 93(4), 832–837. <https://doi.org/10.1021/acs.jchemed.5b00418>
- He, Y., Wu, Y., Fu, J., Gao, Q., & Qiu, J. (2020). Development of 3D printable microfluidic chips with enhanced structural integrity and functional performance. *Micromachines*, 11(7), 667. <https://doi.org/10.3390/mi11070667>
- Hessel, V., Löwe, H., & Schönfeld, F. (2005). Micromixers—a review on passive and active mixing principles. *Chemical Engineering Science*, 60(8–9), 2479–2501. <https://doi.org/10.1016/j.ces.2004.11.033>
- Jensen, K. F. (2001). Microreaction engineering—Is small better? *Chemical Engineering Science*, 56(2), 293–303. [https://doi.org/10.1016/S0009-2509\(00\)00343-X](https://doi.org/10.1016/S0009-2509(00)00343-X)
- Kitson, P. J., Rosnes, M. H., Sans, V., Dragone, V., & Cronin, L. (2012). Configurable 3D-printed millifluidic and microfluidic ‘lab on a chip’ reactionware devices. *Lab on a Chip*, 12(18), 3267–3271. <https://doi.org/10.1039/c2lc40761b>
- Macdonald, N. P., Zhu, F., Hall, C. J., Reboud, J., Crosier, P. S., Patton, E. E., Wlodkowic, D., Cooper, J. M., & Zhang, Y. (2017). Assessment of biocompatibility of 3D printed photopolymers using zebrafish embryo toxicity assays. *Lab on a Chip*, 16(2), 291–297. <https://doi.org/10.1039/C6LC01310J>
- Moeini, F., Ranjbaran, M., Rahimi, M., & Moghaddam, M. A. (2021). Integration of 3D printing and process intensification in chemical reactors: A critical review. *Chemical Engineering and Processing - Process Intensification*, 159, 108246. <https://doi.org/10.1016/j.cep.2020.108246>
- Waheed, S., Cabot, J. M., Macdonald, N. P., Lewis, T., Guijt, R. M., Paull, B., & Breadmore, M. C. (2016). 3D printed microfluidic devices: Enablers and barriers. *Lab on a Chip*, 16(11), 1993–2013. <https://doi.org/10.1039/C6LC00284F>
- Wang, H., Yu, H., Chen, C., & Wang, Y. (2019). Design and optimization of microreactors using computational fluid dynamics. *Micromachines*, 10(9), 628. <https://doi.org/10.3390/mi10090628>
- Wang, L., & Pumera, M. (2021). Recent advances of 3D printing in analytical chemistry: Focus on microfluidic, separation, and extraction devices. *TrAC Trends in Analytical Chemistry*, 135, 116151. <https://doi.org/10.1016/j.trac.2020.116151>